Hindawi
Journal of Chemistry
Volume 2023, Article ID 9819680, 1 page
https://doi.org/10.1155/2023/9819680

Retraction

Retracted: Electrochemical Application of Structured Color Nanotextile Materials in Garment Design

Journal of Chemistry

Received 15 August 2023; Accepted 15 August 2023; Published 16 August 2023

This article has been retracted by Hindawi following an investigation undertaken by the publisher [1]. This investigation has uncovered evidence of one or more of the following indicators of systematic manipulation of the publication process:

(1) Discrepancies in scope

(2) Discrepancies in the description of the research reported

(3) Discrepancies between the availability of data and the research described

(4) Inappropriate citations

(5) Incoherent, meaningless and/or irrelevant content included in the article

(6) Peer-review manipulation

The presence of these indicators undermines our confidence in the integrity of the article's content and we cannot, therefore, vouch for its reliability. Please note that this notice is intended solely to alert readers that the content of this article is unreliable. We have not investigated whether authors were aware of or involved in the systematic manipulation of the publication process.

Wiley and Hindawi regrets that the usual quality checks did not identify these issues before publication and have since put additional measures in place to safeguard research integrity.

We wish to credit our own Research Integrity and Research Publishing teams and anonymous and named external researchers and research integrity experts for contributing to this investigation.

The corresponding author, as the representative of all authors, has been given the opportunity to register their agreement or disagreement to this retraction. We have kept a record of any response received.

References

[1] Z. Zhang, "Electrochemical Application of Structured Color Nanotextile Materials in Garment Design," *Journal of Chemistry*, vol. 2022, Article ID 2044265, 7 pages, 2022.

Hindawi
Journal of Chemistry
Volume 2022, Article ID 2044265, 7 pages
https://doi.org/10.1155/2022/2044265

Research Article

Electrochemical Application of Structured Color Nanotextile Materials in Garment Design

Zekai Zhang

Guangdong Vocational College of Innovation and Technology, Dongguan, Guangdong 523960, China

Correspondence should be addressed to Zekai Zhang; 11231608@stu.wxic.edu.cn

Received 12 July 2022; Revised 29 July 2022; Accepted 2 August 2022; Published 25 August 2022

Academic Editor: K. K. Aruna

In order to improve the color saturation of textile structured chromogenic photonic crystals, this paper proposes that the dye adsorbed PSt structural elements (reactive dyes/PSt microspheres) on the outer surface can be used to construct electrochemically structured chromogenic photonic crystals on mulberry fabrics by digital printing. In this method, the adsorption conditions and adsorption model of dyes on the surface of PSt colloidal microspheres were studied. The structure and morphology of reactive dyes/PSt microspheres, the arrangement of the obtained photonic crystals, and the structural chromogenic effect were characterized. The results showed that the amount of dye adsorbed on the surface of microspheres increased significantly with the increase of adsorption temperature from 25°C to 65°C. When the adsorption temperature continued to rise to 75°C, the dye adsorption capacity on the surface of PSt microspheres did not increase significantly. The adsorption model accords with the Langmuir model; reactive dye/PSt microspheres have a typical core-shell structure, and the particle size of the microspheres is slightly larger than that before adsorption. *Conclusion*. The reactive dye/PSt photonic crystal chromogenic electrochemical structure constructed on the surface of white silk fabric has a regular and orderly arrangement of microspheres, showing bright structural color.

1. Introduction

Textiles are mainly colored by applying dyes or pigments. In recent years, some new textile coloring technologies are emerging. Among them, the construction of photonic crystals on textile substrates, through the diffraction of light and other functions, to obtain the structural color effect to realize the ecological and environmental coloring of textiles has attracted the attention of researchers. As a typical physical color, the structural color produced by regularly arranged crystalline photonic crystals usually has the characteristics of high saturation, high brightness, and rainbow effect, which helps to enrich the pigment color and make the finishing point. However, it is challenging to construct photonic crystal electrochemistry structures on textile substrates to realize textile coloring. Textile is a kind of rough, porous, and flexible material with certain undulation, which can be divided into woven, knitted, and nonwoven kinds according to the weaving method [1]. Different weaving and processing methods will have different effects on the properties of textiles, which brings challenges to the construction of photonic crystal structures on textile substrates. At the same time, it is also difficult to prepare bright and colorful structural color films. Therefore, finding a textile substrate suitable for colloidal microsphere self-assembly to construct regular photonic crystals and obtain bright structural color effect will have good practical significance for realizing textile photonic crystal structure coloring, as shown in Figure 1.

The colloidal microsphere self-assembly method has the advantages of simple operation and good practicability. It is the most widely used method for preparing photonic crystals, mainly including the gravity sedimentation method, vertical sedimentation method, centrifugal deposition method, and electrophoretic deposition method. [2]. However, the above conventional colloidal microspheres self-assembly method has the disadvantages of low efficiency and long time, which greatly inhibits the application of

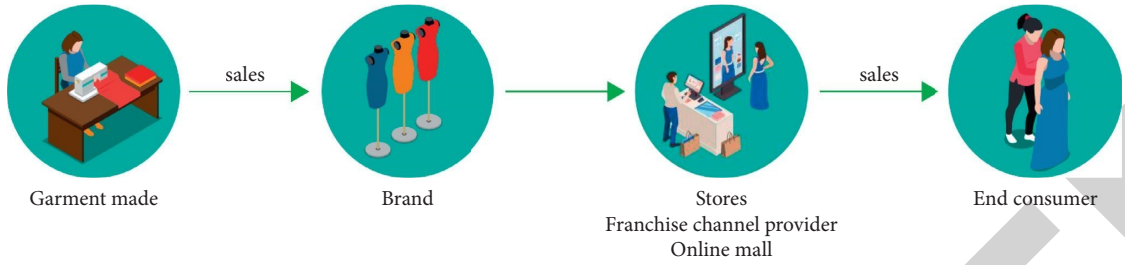

Figure 1: Clothing design process.

photonic crystal structure color in the textile field. Therefore, there is an urgent need to develop a colloidal microsphere self-assembly method that is practical, efficient, and suitable for the preparation of good photonic crystal chromogenic electrochemical structures. As a common method in industrial production, the spraying method has the advantages of simple operation, high efficiency, and low cost and can realize large-area rapid prototyping of materials on the plane and curved surface [3]. If the spraying method and colloidal microsphere self-assembly method can be combined, it is expected to open up a large-area, rapid, and efficient way to prepare photonic crystals, which will help to promote the practical application of photonic crystal structure color. After selecting suitable textile substrates and rapidly constructing the photochromic electrochemical structure of photonic crystals, the stability of the electrochromic structure of photonic crystals will become an important bottleneck restricting the application of the electrochromic structure of photonic crystals [4]. When undergoing simple folding, bending, washing, and friction, the photonic crystal structure is easy to fall off from the substrate and the corresponding structural color effect is easy to be reduced. Therefore, how to improve the stability of the electrochemical structure of photonic crystal color generation and retain the structural color effect is a problem that researchers in the field of photonic crystal structure color generation pay close attention to.

2. Literature Review

Graves et al. added photosensitive pigments and thermal pigments to the spinning solution through electrospinning to prepare electrospun cellulose acetate fiber with corresponding color-changing ability, which filled the research gap of photon sensor in electrospun cellulose acetate (CA) and obtained fabrics with photothermal color changing ability [5]. Guo et al. took carbon nanotube/cotton composite yarn (CCY) as the core and nanofiber polyurethane/temperature sensitive ink as the sheath and prepared skin core nanocomposite yarn with excellent mechanical properties, electrothermal properties, and electrochromic properties; that is, color change will occur when there is a charge on the fabric [6]. J. M. et al. synthesized magnetic nanosphere with magnetochromic ability by the hydrothermal method, mixed it with resin polyethylene glycol diacrylate (PEGDA), and then irradiated it with ultraviolet light to prepare cured color fiber. This magnetochromic dispersion is a kind of magnetochromic material [7]. Duaux et al. reported the preparation of thermochromic cotton fabric, that is, its smart application in children's clothing. However, some challenges still exist. The cost of thermochromic dyes or pigments is particularly high, the durability of thermochromic fibers is poor, and the manufacturing process is complex [8]. Therefore, it is still very necessary to develop a new method for continuously manufacturing thermochromic fibers. Dhiman et al. reported the use of a modular microfluidic system to manufacture alginate microfibers for magnetic response control of drug release and cell culture [9]. Syrek et al. continuously prepared carboxylated chitosan, polyvinyl alcohol, and hydrophobic ethylene vinyl alcohol copolymer (EVOH) spiral microfibers through microfluidic technology. Guo et al. prepared conductive PEDOT: PSS polymer hydrogel microfibers from multiflow microfluidic spinning [10]. Qu et al. used a new buoyancy-assisted vertical microfluidic device to produce a deformable hydrogel microfiber filled with bubbles. However, there are relatively few studies on manufacturing thermochromic fibers by microfluidic spinning [11].

In this paper, the black reactive dye was introduced into the surface of PSt colloidal microspheres by electrostatic adsorption, and the reactive dye/PSt composite colloidal microspheres were prepared. The structured reactive dye/PSt photonic crystals were constructed on mulberry silk fabrics by digital spray printing, showing bright structural colors, in order to provide a reference for the application of structural color and pigment color coupling in textiles.

3. Research Methods

3.1. Experimental Materials and Instruments. Materials used included silk fabric (electric spinning, area density 45.7), commercially available; styrene (st, analytically pure); polyvinylpyrrolidone (PVP, analytically pure); azobisisobutyl ether hydrochloride (AIBA, analytical purity); deionized water (conductivity: 18 m Ω/cm), self-made in the laboratory; water-repellent EPF (industrial grade); and reactive black (industrial grade).

Instruments used were Lambda-35 ultraviolet visible spectrophotometer; Brook-21 zeta potentiometer; Mastersizer-2000 Malvern laser particle sizer; Altra55 field emission scanning electron microscope; Jem2100 transmission electron microscope; 600D digital camera; KH-7700 3D video microscope; Judge-II standard light source box; and 7000 d dialysis bag.

3.2. Sample Preparation Method

3.2.1. Pretreatment of Silk Fabric. In order to prevent the seeping phenomenon in the process of digital jet printing, the mulberry silk fabric was treated with EPF solution with a mass fraction of 1% for two dipping and two rolling processes (the rolling yield was 90%) [12]. The pretreatment of mulberry silk fabric was completed by predrying at 80°C for 3 min and 130°C for 2 min.

3.2.2. Preparation of Reactive Dye/PSt Microspheres. Using the dispersion polymerization method, we weigh 1.5 g of PVP dispersant, 10.0 g of St monomer, and 90.0 g of deionized water, respectively, and add them to the three-necked flask. We place the three-necked flask in a constant temperature water bath for heating and stirring. When the temperature rises to 75°C, we add 0.15 g of AIBA (initiator) dissolved in 10.0 g of deionized water into the three-necked flask and make them react at a constant temperature for 7 hours at a speed of 300 R/min, so as to prepare positively charged PSt microspheres with a particle size of 247 nm [13]. The positively charged PSt colloidal microspheres with good monodispersity (PDI < 0.08) and particle size in the range of 180~350 nm can be prepared by adjusting the amount of monomer and initiator. Reactive black was added to the PSt microsphere lotion of a certain concentration, stirred, and adsorbed at a specific temperature for a certain period of time, and the reactive dye/PSt microsphere was obtained after centrifugal cleaning with deionized water.

3.2.3. Self-Assembly of Reactive Dye/PSt Microspheres by Spray Printing. The reactive dye/PSt colloidal microsphere lotion was sprayed onto the mulberry silk fabric with a desktop dispensing system (the nozzle diameter was 0.15 mm, and the printing pressure was 0.20 MPa). Reactive dye/PSt structure chromogenic photonic crystals can be obtained after the solvent is completely evaporated in a 60°C blast oven.

3.3. Testing and Characterization

3.3.1. Characterization of Physical Properties of Colloidal Microspheres. The average particle size of colloidal microspheres was measured with a Malvin laser particle sizer, and the surface potential of colloidal microspheres was measured with a Zeta potentiometer. The structure and morphology of colloidal microspheres were observed by TEM and FESEM.

3.3.2. Drawing of Adsorption Isotherm and Calculation of Normal Deviation. A UV visible spectrophotometer is used to test the absorbance value at the maximum absorption wavelength of reactive dye solutions with different mass fractions, and the standard working curve of dyes is drawn [14]. We determine the absorbance of dialysate of reactive dye/PSt microspheres, calculate the adsorption amount of dye on the microspheres by Lambert–Beer law, and draw the adsorption rate curve. The deviation between the experimental value and the theoretical value calculated from the adsorption equation is called the normal deviation (ND). By judging the fitting degree between the experimental point and the adsorption model, the calculation formula is as follows:

$$\mathrm{ND} = \left(\frac{1}{N}\right)\left(\frac{\sum_{i=1}^{N} C_{f,1}^{\mathrm{calc}} - C_{f,1}^{\mathrm{exp}}}{C_{f,1}^{\mathrm{exp}}}\right), \quad (1)$$

where $C_{f,i}^{\mathrm{calc}}$ and $C_{f,i}^{\mathrm{exp}}$ are the calculated and experimental values of dye adsorption capacity on the microspheres, respectively, and N is the number of experimental points.

3.3.3. Morphology and Color Characterization of Structured Chromogenic Photonic Crystals. The surface morphology of the structure colored photonic crystals prepared on the fabric was observed by FESEM. The photonic crystal structure color on mulberry silk fabric was observed with a digital camera and three-dimensional video microscope. The reflectance curve of the structured chromogenic photonic crystal constructed on the fabric in the range of 400~700 nm was measured using the UV-Vis spectrophotometer.

4. Result Analysis

4.1. Process Parameters of Reactive Dye/PSt Microspheres

4.1.1. Dye Mass Fraction. During the polymerization of polystyrene, due to the introduction of positive initiator AIBA, the PSt colloidal microspheres synthesized in the experiment are positively charged, which can adsorb anionic reactive dyes [15]. Figure 2 shows the dye adsorption amount on the surface of PSt colloidal microspheres after adsorption at 60°C for 40 min. It can be seen that when the mass fraction of dye is less than 0.5%, the dye adsorption capacity on the surface of PSt microspheres increases significantly with the increase of the amount of dye. When the dye mass fraction was higher than 0.5%, the dye adsorption on the surface of PSt microspheres tended to be saturated and the increment was not obvious. Figure 3 shows the zeta potential curve of PSt microspheres under different dye dosages. It can be seen that the zeta potential of PSt colloidal microspheres is about +30 mV before dye adsorption. When the adsorption amount of reactive dyes increases from 0% to 0.5%, the corresponding zeta potential drops sharply. This should be driven by electrostatic attraction; many reactive dye anions are adsorbed on the surface of PSt microspheres. With the increase of dye mass fraction, the dye adsorption amount on the surface of PSt microspheres also increases. When the dye mass fraction reaches more than 0.5%, the zeta potential of the microsphere lotion tends to be stable, lower than −30 mV, showing good stability [16]. It showed that when the mass fraction of dye reached 0.5%, the adsorption of reactive dye molecules on the surface of PSt microspheres basically reached saturation. To sum up, the appropriate dye mass fraction is determined to be 0.5%.

4.1.2. Adsorption Time. Figure 4 shows the effect of different adsorption time periods on the dye adsorption capacity on the surface of PSt colloidal microspheres at 60°C and 0.5% dye mass fraction.

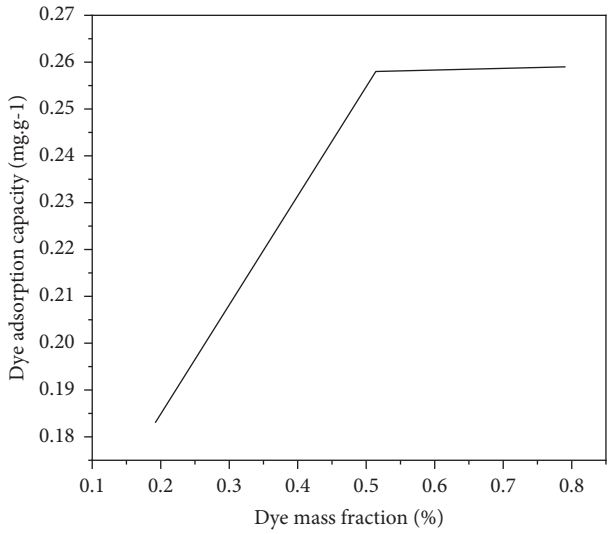

Figure 2: Dye adsorption capacity on the surface of PSt colloidal microspheres under different dye mass fractions.

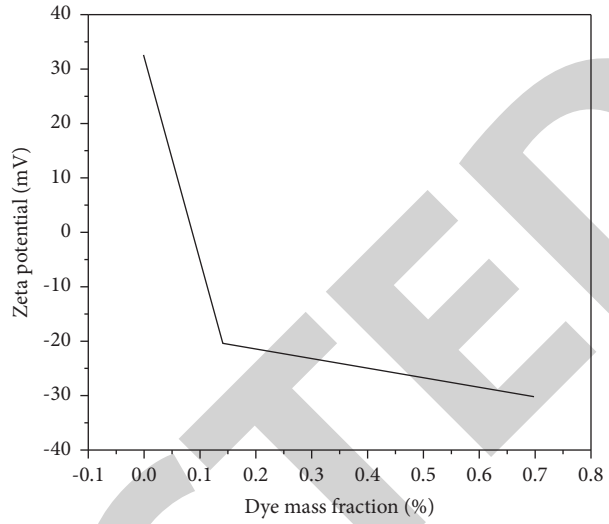

Figure 3: Zeta potential of PSt colloidal microspheres with different dye mass fractions.

It can be seen that in the first 30 minutes of adsorption, the adsorption amount of reactive dyes on the surface of PSt microspheres increased linearly with the extension of adsorption time. If the adsorption time was prolonged, the dye adsorption capacity increased slowly. When the adsorption time was more than 40 min, the adsorption amount of dye did not increase significantly with the extension of adsorption time. This is mainly because, in the initial adsorption stage, there are a large number of positive charges on the surface of PSt microspheres, which makes a large number of anionic reactive dyes quickly adsorb to the surface of the microspheres; With the prolongation of adsorption time, the adsorption of anionic reactive dyes gradually reduced the positive electricity of the surface of the microspheres, and the subsequent increase in the amount of dye adsorption tended to moderate. In the later stage, the adsorption time continues to be extended, and the adsorption amount gradually reaches saturation and remains basically unchanged [17]. In conclusion, 40 min is a more suitable adsorption time.

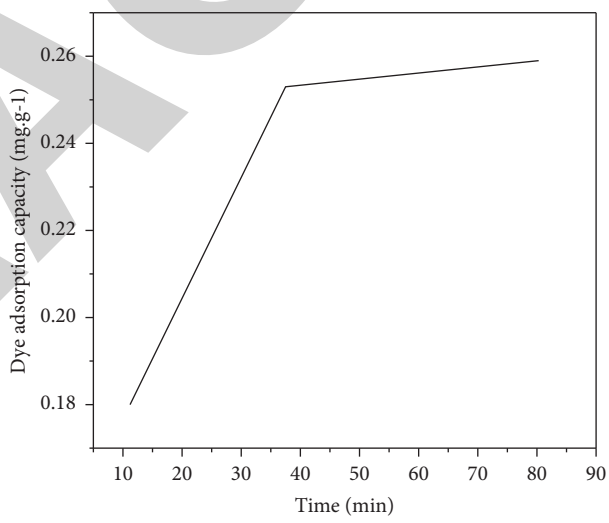

Figure 4: Dye adsorption amount on the surface of PSt colloidal microspheres at different adsorption time periods.

4.1.3. Adsorption Temperature. Figure 5 shows the effect of different adsorption temperatures on the dye adsorption capacity of PSt colloidal microspheres when the dye mass fraction is 0.5% and the adsorption time is 40 min.

It can be seen from Figure 5 that the dye adsorption amount on the surface of microspheres increased significantly with the increase of adsorption temperature from 25°C to 65°C. When the adsorption temperature continued to rise to 75°C, the dye adsorption on the surface of PSt microspheres did not increase significantly. This is because the higher the adsorption temperature is, the more intense the Brownian motion of reactive dye molecules and PSt microspheres becomes. The faster the reactive dye diffuses to the surface of microspheres, the more the dye adsorbed on the surface of microspheres. However, increasing the adsorption temperature will also accelerate the desorption rate of reactive dye on the surface of microspheres [18]. According to the comprehensive analysis, the adsorption temperature should be kept at about 65°C.

4.2. Adsorption Model of Dyes on PSt Colloidal Microspheres. In order to improve the controllability of the adsorption of reactive dyes on the surface of PSt colloidal microspheres and provide better theoretical guidance for its process optimization, the adsorption model of reactive dyes on the surface of PSt colloidal microspheres was further studied. Under the conditions of dye mass fraction of 0.5% and adsorption time of 40 min, the adsorption isotherms of reactive dyes on the surface of PSt colloidal microspheres at 25°C, 45°C, and 65°C were plotted. Three common theoretical adsorption models (Nernst, Langmuir, and Freundlich) were used to fit the adsorption

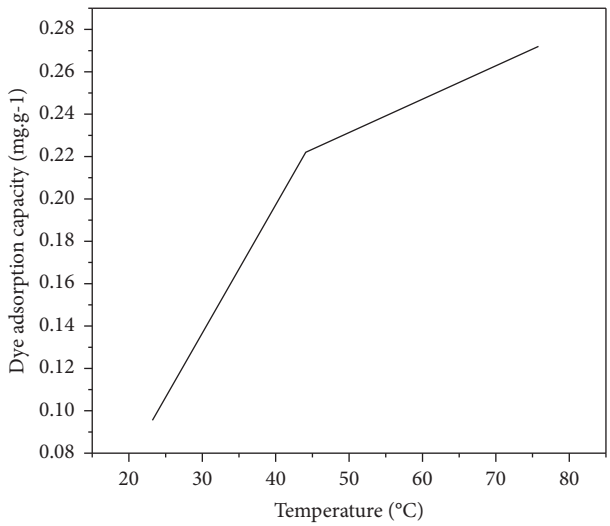

Figure 5: Dye adsorption capacity of PSt colloidal microspheres at different adsorption temperatures.

isotherms at different temperatures by the nonlinear least square method.

By comparing the corresponding normal deviation and fitting coefficient, the conformity degree of the three adsorption models is analyzed (see Table 1). The specific adsorption equation is shown in equations (2) to (4).

4.2.1. Nernst Type

$$[D]_f = K_1 [D]_s. \quad (2)$$

Here, $[D]_f$ is the concentration of dye on the fiber; $[D]_s$ is the concentration of the dye in the dye solution; and K_1 is the Nernst adsorption constant.

4.2.2. Langmuir Type

$$[D]_f = \frac{K_2 [D]_s [S]_f}{1 + K [D]_s}. \quad (3)$$

Here, K_2 is Langmuir adsorption constant and $[S]_f$ is the dyeing saturation value of the fiber.

4.2.3. Freundlich Type

$$[D]_f = K_3 [D]_s^n. \quad (4)$$

Here, K_3 is Freundlich adsorption constant and n is the heterogeneity factor, $0 < n < 1$.

It can be seen from Table 1 that under three different temperatures, the R^2 of Nernst type and Freundlich type are low and the ND is large. The Langmuir model has the highest R^2 , which is more than 0.99, and the corresponding ND is also the lowest [19]. Therefore, the adsorption model of reactive dyes on PSt colloidal microspheres is more in line with the Langmuir model. It can be seen that reactive dyes are localized on the surface of PSt microspheres. That is, a certain number of adsorption sites are formed on the surface

Table 1: Simulation results of adsorption isotherms of reactive dyes on PSt colloidal microspheres.

Temperature/°C	Nernst model		Langmuir model		Freundlich model	
	ND%	R^2	ND%	R^2	ND%	R^2
25	36.2	0.853	4.1	0.990	17.0	0.943
45	40.6	0.832	2.3	0.994	17.5	0.943
65	27.1	0.904	1.1	0.997	13.8	0.968

of positively charged PSt colloidal microspheres, which promotes the localized adsorption of anionic reactive dyes, and there is an adsorption saturation value in the adsorption process. When the adsorption reaches a certain degree, the adsorption amount basically remains unchanged.

4.3. Apparent Morphology of Reactive Dye/PSt Microspheres. From the SEM and TEM photos before and after dye adsorption on the surface of PSt microspheres, it can be concluded that after dye adsorption, the reactive dye/PSt microspheres still maintain a typical core-shell structure and the sphericity is still good. The dye adsorption has no significant effect on the sphericity of colloidal microspheres. However, after adsorption of dyes, the particle size of reactive dye/PSt microspheres increased from 184.5 nm to 196.3 nm and the shell thickness increased from 30.7 nm to 36.6 nm. This may be because a large number of dye molecules are adsorbed on the surface of PSt microspheres, which can adsorb a certain amount of water molecules at the same time, resulting in a slight increase in the particle size of the microspheres.

4.4. Application of Reactive Dye/PSt Microspheres. From the self-assembled photonic crystal structures and corresponding structural colors of reactive dyes/PSt microspheres with different particle sizes on mulberry silk fabrics, it can be concluded that the structures of reactive dyes/PSt photonic crystals on mulberry silk fabrics are orderly arranged, showing uniform and bright structural colors; And with the decrease of the particle size of colloidal microspheres, the corresponding structural colors also show different hues such as red, orange, green, blue, and purple, and an obvious blue shift occurs [6].

Reflectivity Curves of Self-Assembled Photonic Crystals with Different Particle Sizes of Reactive Dye/PSt Microspheres on White Mulberry Silk Fabric. It can be seen that as the particle size of the reactive dye/PSt microspheres decreases from 317, 298, 247, and 201 nm to 188 nm, the maximum reflection wavelength of the structure-colored photonic crystal gradually changes from 615 nm to 418 nm, which corresponds to the color phenomenon of the self-assembled photonic crystal structure of reactive dye/PSt microspheres with different particle sizes sprayed on mulberry fabric, that is, there is an obvious blue shift, which conforms to the Bragg diffraction equation.

Before dye adsorption, the structure color of pure PSt microspheres on white mulberry silk fabric was dim, showing light blue and light green. After adsorbing the dye,

the reactive dye/PSt photonic crystal on the same substrate shows bright blue and green and the corresponding color saturation is significantly improved. This is because the white fabric can easily reflect almost all the incident light passing through the photonic crystal layer without selectivity, diluting the structural color of the selective reflection of the photonic crystal. The black dye can significantly absorb the background stray light and make the light reflected by the photonic crystal maintain good purity and saturation without the interference of additional light [20]. The results show that the structure color effect of reactive dye/PSt photonic crystal on white mulberry silk fabric is better than that of pure PSt photonic crystal. It can be concluded that the introduction of black reactive dyes into the surface of PSt microspheres to prepare composite structural units can effectively enhance the color saturation of the structure chromogenic photonic crystals on the white substrate.

5. Conclusion

(1) In this paper, reactive dye/polystyrene (PSt) composite colloidal microspheres were prepared by electrostatic adsorption. The optimum conditions for dye adsorption were determined: dye mass fraction was 0.5%, adsorption temperature was 65°C, and adsorption time was 40 min.

(2) The adsorption of active black B on positively charged PSt colloidal microspheres conforms to the Langmuir model and belongs to localized adsorption.

(3) Using the digital spray printing method and the reactive dye/PSt composite colloidal microspheres as the structural elements, the structured three-dimensional photonic crystals can be directly constructed on the white mulberry silk fabric, showing bright and beautiful structural colors, which have certain reference significance for the application of the coupling of structural colors and pigment colors in textiles.

Data Availability

The data used to support the findings of this study are available from the author upon request.

Conflicts of Interest

The author declares no conflicts of interest.

Acknowledgments

This work was supported by the Guangdong Vocational College of Innovation and Technology, Application Research of Intangible Cultural Heritage Bead Embroidery Techniques into the Course of "Fundamentals of Fashion Design" (Number: CXJGKT20212299).

References

[1] Z. A. Razak, S. A. Rushdi, M. Y. Gadhban, S. Al-Najjar, and Z. T. Al-Sharify, "Possibility of utilizing the lemon peels in removing of red reactive (rr) dye from simulated aqueous solution," *International Journal of Green Energy*, vol. 10, no. 10, pp. 7343–7359, 2020.

[2] M. Pająk and A. Dzieniszewska, "Evaluation of the metallurgical dust sorbent efficacy in reactive blue 19 dye removal from aqueous solutions and textile wastewater," *Environmental Engineering Science*, vol. 37, no. 7, pp. 509–518, 2020.

[3] D. M. Lewis, P. J. Broadbent, C. M. Carr, and W. D. He, "Investigation into the reaction of reactive dyes with carboxylate salts and the application of carboxylate-modified reactive dyes to cotton," *Coloration Technology*, vol. 138, no. 1, pp. 58–70, 2022.

[4] S. Bapat, D. Jaspal, and A. Malviya, "Efficacy of parthenium hysterophorus waste biomass compared with activated charcoal for the removal of ci reactive red 239 textile dye from wastewater," *Coloration Technology*, vol. 137, no. 3, pp. 234–250, 2021.

[5] L. S. Graves, M. J. Goodwin, I. N. Maricar, J. A. Rebstock, and E. J. Harbron, "Maximizing amplified energy transfer: tuning particle size and dye loading in conjugated polymer nanoparticles," *Journal of Physical Chemistry C*, vol. 124, no. 48, pp. 26474–26485, 2020.

[6] Q. Guo, W. Chen, Z. Cui, and H. Jiang, "Reactive dyeing of silk using commercial acid dyes based on a three-component mannich-type reaction," *Coloration Technology*, vol. 136, no. 4, pp. 336–345, 2020.

[7] J. M. He, C. F. Xie, and J. J. Long, "Sustainable color stripping of cotton substrate dyed with reactive dyes in a developed uv/k2s2o8 photocatalytic system," *Journal of the Taiwan Institute of Chemical Engineers*, vol. 121, no. 2, pp. 241–256, 2021.

[8] G. Duaux, E. Fleury, and D. Portinha, "Biobased poly(ester-*co*-glycoside) from reactive natural Brønsted acidic deep eutectic solvent analogue," *Polymer Chemistry*, vol. 12, no. 38, pp. 5485–5494, 2021.

[9] G. Dhiman, V. Vinoth Kumar, A. Kaur, and A. Sharma, "Don: deep learning and optimization-based framework for detection of novel coronavirus disease using x-ray images," *Interdisciplinary Sciences: Computational Life Sciences*, vol. 13, no. 2, pp. 260–272, 2021.

[10] K. Syrek, A. Sennik-Kubiec, J. Rodríguez-López et al., "Reactive and morphological trends on porous anodic tio 2 substrates obtained at different annealing temperatures," *International Journal of Hydrogen Energy*, vol. 45, no. 7, pp. 4376–4389, 2020.

[11] Y. Qu, P. Li, P. Hou, Q. Wang, and S. Luo, "Controllable synthesis of polystyrene microspheres used as template and in-situ carbon source for li2mnsio4 cathode material to boost lithium-ion batteries performance," *International Journal of Energy Research*, vol. 46, no. 2, pp. 1711–1721, 2022.

[12] S. Shriram, B. Nagaraj, J. Jaya, S. Shankar, and P. Ajay, "Deep learning-based real-time AI virtual mouse system using computer vision to avoid COVID-19 spread," *Journal of Healthcare Engineering*, vol. 2021, Article ID 8133076, 8 pages, 2021.

[13] W. He, X. H. Dong, J. G. Zhou, and M. K. Fung, "Manipulation of the size of polystyrene spheres as the templates for internal light out-coupling structures of a white organic light-emitting diode," *Journal of Materials Chemistry C*, vol. 9, no. 21, pp. 6923–6929, 2021.

[14] J. Chen, J. Liu, X. Liu, X. Xu, and F. Zhong, "Decomposition of toluene with a combined plasma photolysis (cpp) reactor: influence of uv irradiation and byproduct analysis," *Plasma Chemistry and Plasma Processing*, vol. 41, no. 1, pp. 409–420, 2020.

[15] A. Verdianto, H. Lim, J. G. Kang, and S. Kim, "Scalable, colloidal synthesis of snsb nanoalloy-decorated mesoporous 3d nio microspheres as a sodium-ion battery anode," *International Journal of Energy Research*, vol. 46, no. 4, pp. 4267–4278, 2022.

[16] Z. Huang and S. Li, "Reactivation of learned reward association reduces retroactive interference from new reward learning," *Journal of Experimental Psychology Learning Memory and Cognition*, vol. 48, no. 2, pp. 213–225, 2022.

[17] Y. T. Wang, R. N. Wu, C. C. Ni et al., "Important role of surface plasmon coupling with the quantum wells in a surface plasmon enhanced color-converting structure of colloidal quantum dots on quantum wells," *Optics Express*, vol. 28, no. 9, pp. 13352–13367, 2020.

[18] N. Chen, Z. X. Wang, H. Chen et al., "Magnetic interference gonioapparent thin film based on metal-dielectric-metal structure for optical security devices," *Optoelectronics Letters*, vol. 16, no. 2, pp. 97–102, 2020.

[19] R. Huang and X. Yang, "Analysis and research hotspots of ceramic materials in textile application," *Journal of Ceramic Processing Research*, vol. 23, no. 3, pp. 312–319, 2022.

[20] Q. Zhou, W. Wu, and T. Xing, "Study on the mechanism of laccase-catalyzed polydopamine rapid dyeing and modification of silk," *RSC Advances*, vol. 12, no. 6, pp. 3763–3773, 2022.